

Reaction Rates and Mechanisms of the Formation of Gallium(III), Indium(III), and Thallium(III) Complexes with Semi-Xylenol Orange in Aqueous Solutions

Yoichi KAWAI, Tetsuro TAKAHASHI,* Katsuyuki HAYASHI,** Taira IMAMURA, Hiroaki NAKAYAMA,*** and Masatoshi FUJIMOTO

Department of Chemistry, Faculty of Science, Hokkaido University, Sapporo

(Received September 6, 1971)

The kinetics for the complex formation of Ga(III), In(III), and Tl(III) with Semi-Xylenol Orange (SXO) in acid solutions were studied by stopped-flow technique. Kinetic results are interpreted in terms of a two-step mechanism involving pre-equilibrium. The increase in the reaction rate with decreasing hydrogen ion concentration is interpreted as the sum of several parallel pathways including monohydroxo metal ions and a few charge types of the ligand. The mechanisms and the rates of the three different d^{10} -system metal ions are discussed. The phenomena of the slower increase in absorbance of Ga(III)-SXO complex after the rapid increase and the slow color fading of Tl(III)-SXO complex are also discussed.

Although there have been a large number of investigations on the kinetics of metal complex formation in aqueous solutions,^{1,2)} relatively meager kinetic data have been reported for trivalent d^{10} -system metal ions.³⁻⁶⁾ This arises mainly from the limited number of simple inorganic or organic ligands suitable for kinetic measurements for Ga(III), In(III), and Tl(III).

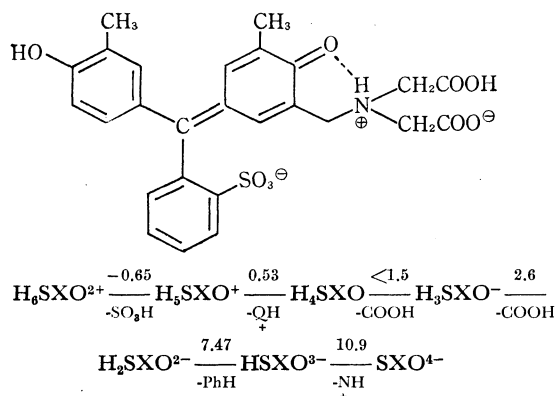


Fig. 1. Semi-Xylenol Orange (SXO) in the form of $[\text{H}_5\text{SXO}]^-$ and the acid dissociation constants ($\text{p}K_a$).¹⁰⁾

* Present address: Yoshitomi Pharmaceutical Industries, Ltd., Osaka.

** Present address: Nisso Smelting Co., Bandai, Fukushima.

*** Present address: Kagawa Nutrition College, Sakado-machi, Saitama.

1) M. Eigen, *Pure Appl. Chem.*, **6**, 97 (1963).

2) A. McAuley and J. Hill, *Quart. Rev.*, **23**, 18 (1969).

3) G. Geier, *Ber. Bunsenges. Physik. Chem.*, **69**, 617 (1965).

4) J. Miceli and J. Stuehr, *J. Amer. Chem. Soc.*, **90**, 6967 (1968).

5) D. Fiat and R. E. Connick, *ibid.*, **88**, 4754 (1966).

6) N. D. Lukomskaya, T. V. Malikova, and K. B. Yatsimirskii, *Zh. Neorg. Khim.*, **12**, 2462 (1967).

In the present study, Semi-Xylenol Orange (SXO) has been chosen as a ligand, which forms 1:1 complexes with Ga(III), In(III), and Tl(III). The SXO complexes have absorption maxima in the visible range with sufficiently large absorption coefficients (see Fig. 1).

Characteristic rate constants for the water substitution in the inner coordination sphere of aquo-ions are listed¹⁾ as 10^0 – 10^1 , $10^{1.5}$ – $10^{2.5}$, and 10^4 – 10^5 sec^{-1} for Ga(III), In(III), and Tl(III), respectively. These are obtained only from the extrapolation of the rate data for other charge types, by assuming that $\log k$ (k : rate constant) correlates linearly with the inverse of ionic radius for non-transition group and d^{10} -system ions. Though divalent d^{10} -metal ions were reported to satisfy the correlation, trivalent d^{10} -metal ions do not necessarily behave in the similar way, as is seen for the correlation of ionization potential and hydration energy with ionic radius.⁷⁾

Experimental

Materials. The solution of Ga(III) perchlorate was prepared by dissolving metallic gallium (99.99% Wako) in perchloric acid (Reagent Grade, Wako). Aqueous In(III) perchlorate was prepared by dissolving indium oxide (Koso) in slight excess of perchloric acid. Aqueous Tl(III) perchlorate was made by electrolytically oxidizing Tl(I) perchlorate⁸⁾ which was prepared from thallium(I) acetate (BDH) and recrystallized.

7) Within a non-transition group the heat of hydration and the ionization potential vary inversely with the ionic radius. Crystal field correction acts well for the first transition series. On the other hand the correlation is almost worth nothing for trivalent d^{10} -system ions.

8) G. Biedermann, *Arkiv Kemi*, **5**, 441 (1953).

The concentration of each metal ion in the stock solution was standardized by titrating with EDTA.⁹⁾

Sodium perchlorate (Reagent Grade, Koso) was dissolved in distilled water. In order to remove the trace amounts of impurities the concentrated aqueous solution was filtered through a quantitative filter paper after being kept several days. The concentration was determined by passing an aliquot of the solution through a column of cation-exchange resin (Dowex 50W-X8) in the hydrogen form and titrating the effluent with standard sodium hydroxide.

SXO was synthesized from *o*-Cresol Red, iminodiacetic acid and formaldehyde by the Mannich condensation and purified by means of cellulose column chromatography.¹⁰⁾ The acid form of SXO was obtained by passing the fraction of SXO through a column of cation-exchange resin in the hydrogen form. The purity of the SXO was checked by paper chromatography, and only one spot was observed. The elemental analysis agrees with the results of the previous workers.¹⁰⁾

Found: C, 56.22; H, 5.39; N, 2.24; S, 4.90%. Calcd for $C_{26}H_{25}O_9NS \cdot H_2O$: C, 57.24; H, 4.99; N, 2.57; S, 5.89%.

Procedure. A Hitachi spectrophotometer model EPS-3T was used for spectral measurements. Yanagimoto SPS-1 Stopped-Flow apparatus with a 4-jet mixing chamber and 2 mm or 10 mm optical cell was used for kinetic measurements. The changes in absorbance were photographed on the storage screen of oscilloscope.

All measurements were made at $25.0 \pm 0.2^\circ\text{C}$. Hydrogen ion concentration and ionic strength were adjusted using HClO_4 and NaClO_4 . The pH values were measured with a Horiba pH meter Model P calibrated with a standard buffer solution.

Results

Two forms of complexes of SXO with the metals M(III) were observed in the different pH region by the spectroscopic measurements. The composition of these complexes in solutions was determined to be 1:1 by means of the continuous variation method. Absorption maxima of the acid-form complexes are at 532 nm (pH=1.60), 529 nm (pH=3.10) and 538 nm ($[\text{H}]=1.0\text{M}$) for Ga(III), In(III), and Tl(III), respectively, and those of the alkaline-form complexes are at 470 nm (pH=4.0), 480 nm (pH=4.50), and 492 nm (pH=6.0) for Ga(III), In(III), and Tl(III), respectively. In order to minimize hydrolysis and polymerization of the metal ions, kinetic measurements were performed in the acid media by following the absorbance at the λ_{max} of the acid-form complex.

When metal(III) ion concentrations were at least in 10-fold excess over those of SXO, a pseudo-first-order kinetics was obeyed in most cases. Pseudo-first-order rate constants k_{obs} were evaluated from the slopes of such plots as

$$k_{\text{obs}} = -d \ln (D_{\infty} - D_t) / dt$$

where D_{∞} and D_t represent the absorbances at the end of the reaction and at time t respectively. No significant dependence was observed for k_{obs} on the initial concentration of SXO. Plots of the observed pseudo-

9) G. Schwarzenbach and H. Flaschka, "Die Komplexmtrische Titration," 5th ed., F. Enke, Stuttgart (1965).

10) M. Murakami, T. Yoshino, and S. Harasawa, *Talanta*, **14**, 1293 (1967).

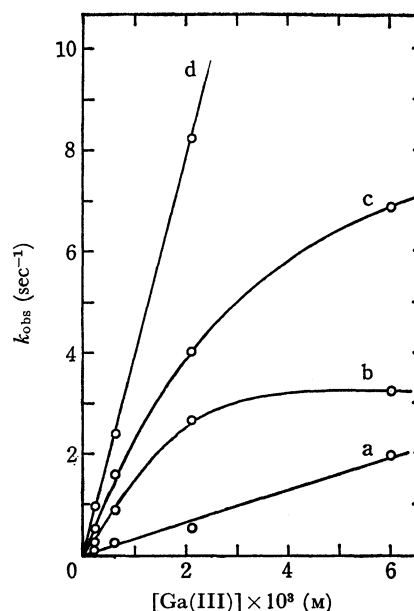


Fig. 2. Plot of k_{obs} vs. total concentration of Ga(III) at various hydrogen ion concentrations, 25.0°C and ionic strength of 0.1.

(a): pH=2.00 \pm 0.02; (b): pH=2.40 \pm 0.02; (c): pH=2.65 \pm 0.02; (d): pH=2.90 \pm 0.02.

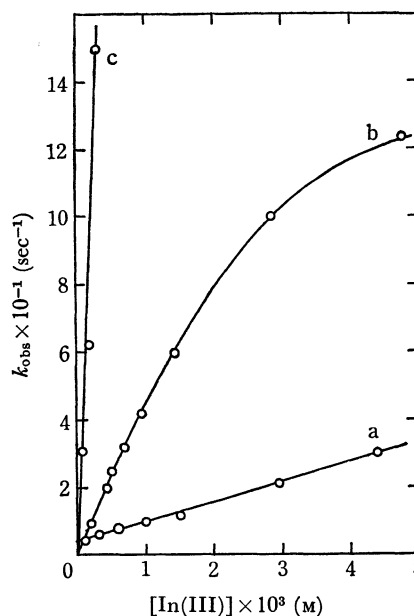
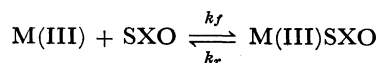


Fig. 3. Plot of k_{obs} vs. total concentration of In(III) at various hydrogen ion concentrations, 25.0°C and ionic strength of 0.1.

(a): pH=1.37 \pm 0.02; (b): pH=1.96 \pm 0.02; (c): pH=3.00 \pm 0.02.

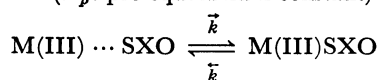
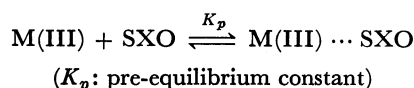
first-order rate constant k_{obs} against $[\text{M(III)}]$ for Ga(III) and In(III) are not straight lines but curves (Figs. 2 and 3). Assuming the one step mechanism such plots should give a straight line with a slope k_f and an intercept k_r ,



$$k_{\text{obs}} = k_f[\text{M(III)}] + k_r \quad (1)$$

The curves can thus be interpreted in terms of the two-

step mechanisms.



Since the metal ion is in large excess over SXO, and is regarded as constant during the reactions, k_{obs} can be written as a function of $[\text{M(III)}]$

$$k_{\text{obs}} = \frac{\bar{k}K_p[\text{M(III)}]}{1 + K_p[\text{M(III)}]} + \bar{k} \quad (2)$$

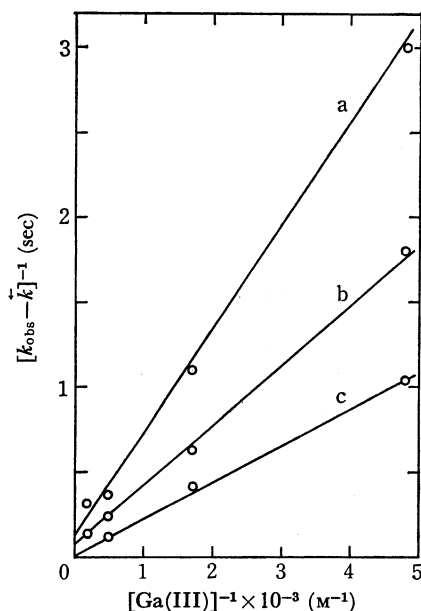


Fig. 4. Plot of $1/(k_{\text{obs}} - \bar{k})$ vs. inverse of the total concentration of Ga(III) for Ga(III)-SXO at various hydrogen ion concentrations.

(a): pH = 2.40 ± 0.02 ; (b): pH = 2.65 ± 0.02 ; (c): pH = 2.90 ± 0.02 .

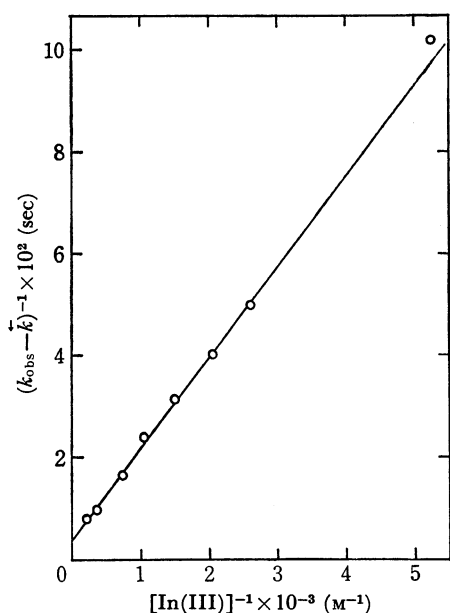


Fig. 5. Plot of $1/(k_{\text{obs}} - \bar{k})$ vs. inverse of the total concentration of In(III) for In(III)-SXO at pH = 1.96 ± 0.02 .

Figures 4 and 5 show a linear plot of $1/(k_{\text{obs}} - \bar{k})$ versus $1/[\text{M(III)}]$ for Ga(III) and In(III) respectively. We have for the present no evidence of the actual structure of the intermediate $\text{M(III)} \cdots \text{SXO}$; it may or may not be so-called ion pair.

If the M(III) concentration is sufficiently low, namely $1 \gg K_p[\text{M(III)}]$, Eq. (2) is reduced to Eq. (1) (namely $\bar{k}K_p = k_f$ and $\bar{k} = k_r$), and the plot of k_{obs} versus $[\text{M(III)}]$ becomes linear. Actually in the case of Tl(III), plots of k_{obs} against $[\text{Tl(III)}]$ were linear under the experimental condition (Fig. 6).

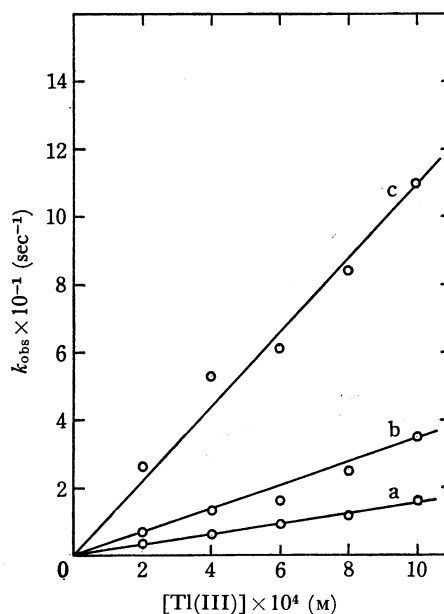
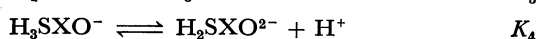
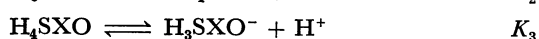
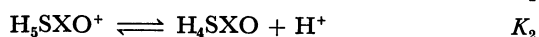
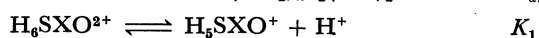
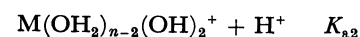
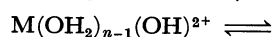
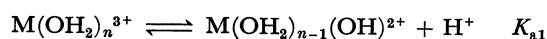


Fig. 6. Plot of k_{obs} vs. total concentration of Tl(III) at 25.0°C , ionic strength 2.0 and at various hydrogen ion concentrations.

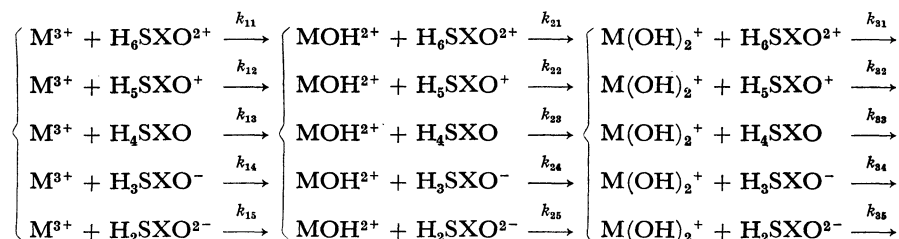
(a): $[\text{H}] = 0.5\text{M}$; (b): $[\text{H}] = 0.3\text{M}$; (c): $[\text{H}] = 0.1\text{M}$.

In the present work the values of k_f for Ga(III), In(III), and Tl(III) are discussed. It is difficult to discuss k_r , as the plots of k_{obs} versus $[\text{M(III)}]$ have intercepts almost near the origin in most cases. This is consistent with the large value of apparent stability constants $K_c = [\text{M(III)SXO}]/[\text{M(III)}][\text{SXO}]$. The apparent stability constants are $1.4 \times 10^5\text{M}$ (pH = 2.1), $1.0 \times 10^5\text{M}$ (pH = 3.0), and $7.9 \times 10^5\text{M}$ ($[\text{H}] = 5 \times 10^{-2}\text{M}$) for Ga(III), In(III), and Tl(III), respectively.

The increase of k_f with decreasing $[\text{H}]$ is interpreted by considering the acid dissociation of aquo ion M^{3+} and SXO.



All the possible chemical species and equilibria are summarized above, polynuclear hydroxo complexes being neglected under the experimental conditions.¹²⁾ Second-order rate constants are defined as follows:



The proton transfer of SXO was found to proceed fast as compared to the complex formation, as in the time range of complex formation no relaxation was observed by the pH-jump on mixing SXO with perchloric acid. The hydrolysis of M(III) is known to be fast as compared to the complex formation reactions.¹¹⁾ Acid dissociation constants of SXO were reported to be $10^{-0.65}$, $10^{-0.53}$, $10^{-1.5}$, and $10^{-2.6}$ for K_1 , K_2 , K_3 , and K_4 respectively (0.1M KNO_3 , 25°C).¹⁰⁾

Ga(III)-SXO. The acid dissociation constants of Ga(III) are reported to be $K_{a1}=10^{-2.8}$ and $K_{a2}=10^{-3.5}$ ($I \rightarrow 0$, 18°C).¹²⁾ H_4SXO , H_3SXO^- , and $\text{H}_2\text{SXO}^{2-}$ are predominant charge types of the ligand under the experimental conditions. The contribution of $\text{Ga}(\text{OH})_2^+$ was neglected. Following equation expresses k_f .

$$k_f = \frac{[k_{13}[\text{H}]^3 + (k_{14}K_3 + k_{23}K_{a1})[\text{H}]^2 + (k_{15}K_3K_4 + k_{24}K_3K_{a1})[\text{H}] + k_{25}K_3K_4K_{a1}]}{([\text{H}] + K_{a1}) \times ([\text{H}]^2 + K_3[\text{H}] + K_3K_4)}$$

In the Fig. 7 $k_f \times ([\text{H}] + K_{a1})([\text{H}]^2 + K_3[\text{H}] + K_3K_4)$ is plotted against $[\text{H}]$ ¹³⁾ to give a straight line. The linearity can be interpreted by assuming that the rate constants k_{25} , and k_{24} and/or k_{15} are sufficiently larger than the others. The term of $k_{25}K_3K_4K_{a1}$ corresponds to the intercept, and the term of $(k_{15}K_3K_4 + k_{24}K_3K_{a1})$ to the slope of the plots, so that the values of k_{15} and

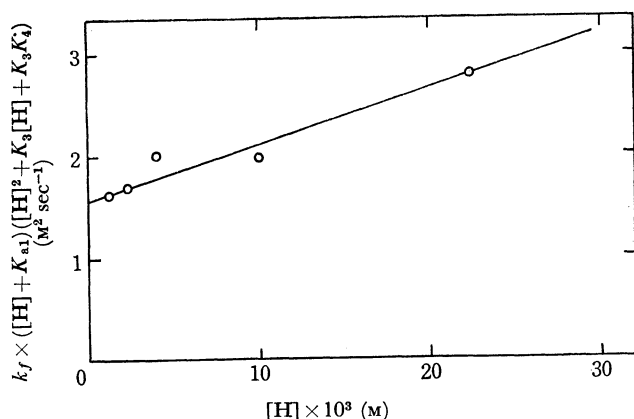


Fig. 7. Plot of $k_f([H] + K_{a1})([H]^2 + K_3[H] + K_3K_4)$ vs. hydrogen ion concentration for Ga(III)-SXO at 25.0°C and ionic strength of 0.1.

11) P. Hemmes, L. D. Rich, D. L. Cole, and E. M. Eyring, *J. Phys. Chem.*, **74**, 2859 (1970).

12) L. G. Sillén and A. E. Martell ed., "Stability Constants", Special Publication No. 17, The Chemical Society, London (1964).

13) Hydrogen ion concentrations $[\text{H}]$ were calculated directly from the observed values of pH without correction of activity coefficients.

k_{24} are indistinguishable.^{14,15)} Following values of k_{15} and k_{24} have been calculated by attributing the slope only to the term $k_{15}K_3K_4$ and to $k_{24}K_3K_{a1}$ respectively: $k_{15}=6.9 \times 10^3 \text{M}^{-1}\text{sec}^{-1}$ and $k_{24}=1.1 \times 10^3 \text{M}^{-1}\text{sec}^{-1}$. From the intercept k_{25} is obtained as $1.2 \times 10^4 \text{M}^{-1}\text{sec}^{-1}$.

In the case of Ga(III), we shall have to refer to the relatively slow increase in optical density. Exponential changes of optical density was really observed on the oscilloscope as mentioned above, but the absorbance of the complex usually still increases gradually even 2 hr after mixing. Under the extreme condition of high pH and high Ga(III) concentration, exponential signal was not observed as shown in Fig. 8.

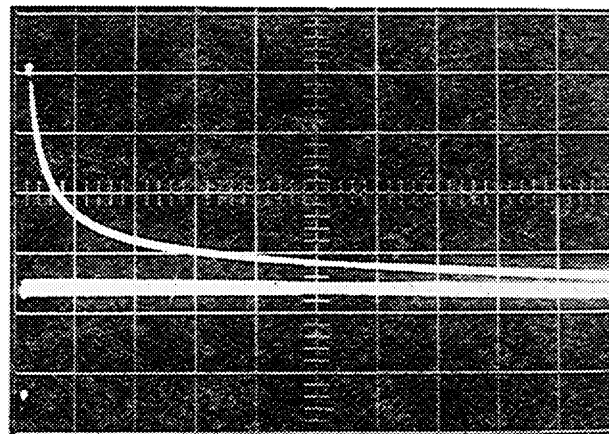


Fig. 8. Stopped-flow signal at 532 nm under the condition of $[\text{Ga(III)}]_0=6.0 \times 10^{-3}\text{M}$, $[\text{SXO}]_0=2.0 \times 10^{-5}\text{M}$, ionic strength 0.1, pH=2.9 and 25.0°C ; vertical scale: absorbance 0.1/div; horizontal scale: 500 msec/div.

In(III)-SXO. The acid dissociation constants of In(III) are reported to be $K_{a1}=10^{-4.4}$ and $K_{a2}=10^{-3.9}$ (3M NaClO_4 , 25°C).¹²⁾ Under the experimental conditions, $\text{In}(\text{OH})_2\text{OH}$ is the predominant chemical species of In(III), and H_4SXO , H_3SXO^- , and $\text{H}_2\text{SXO}^{2-}$ are the predominant charge types of SXO. If the increase of k_f with decreasing $[\text{H}]$ is attributed to the three charge types of the ligand, k_f is expressed as

$$k_f = \frac{k_{13}[\text{H}]^2 + k_{14}K_3[\text{H}] + k_{15}K_3K_4}{[\text{H}]^2 + K_3[\text{H}] + K_3K_4}$$

The plot of $k_f \times ([\text{H}]^2 + K_3[\text{H}] + K_3K_4)$ against $[\text{H}]$ should show a second order increase, but shows a decrease as shown in Fig. 9. Therefore the reaction mechanism involving only $\text{In}(\text{OH})_2\text{OH}$ should be excluded, and the hydrolysis of $\text{In}(\text{OH})_2\text{OH}$ must be taken into account. The rate constant k_f is expressed

14) P. Seewald and N. Sutin, *Inorg. Chem.*, **2**, 643 (1963).

15) D. W. Carlyle and J. H. Espenson, *ibid.*, **6**, 1370 (1967).

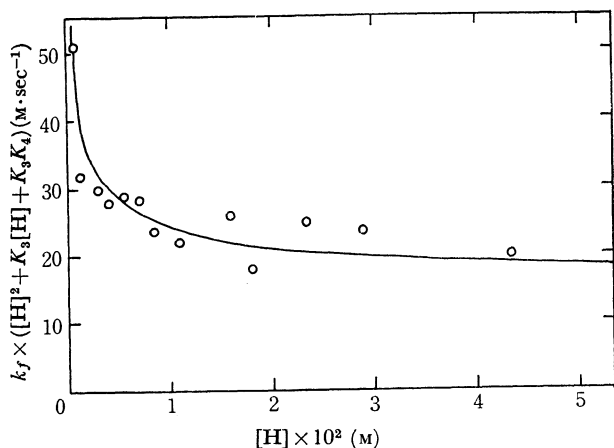


Fig. 9. Plot of $k_f([H]^2 + K_3[H] + K_3K_4)$ vs. hydrogen ion concentration for In(III)-SXO at 25.0°C and ionic strength 0.1.

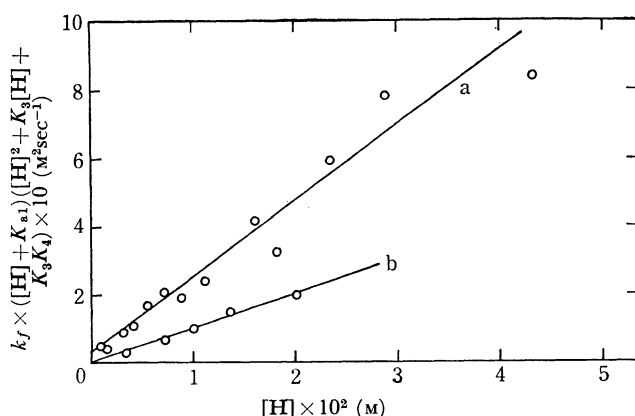


Fig. 10. Plot of $k_f([H] + K_{a1})([H]^2 + K_3[H] + K_3K_4)$ vs. hydrogen ion concentration for In(III)-SXO at 25.0°C and ionic strength 0.1 (a) and 2.0 (b).

by the same equation as given for Ga(III). In Fig. 10, $k_f \times ([H] + K_{a1})([H]^2 + K_3[H] + K_3K_4)$ is plotted against $[H]$. The linearity of the plot is also interpreted by the same assumption as made for Ga(III). The values of k_{25} , k_{24} , and k_{15} are 3.1×10^6 , 5.0×10^6 , and $2.8 \times 10^5 \text{ M}^{-1}\text{sec}^{-1}$ respectively.

In the case of In(III), absorbance of the complex, remains constant for more than 24 hr.

Tl(III)-SXO. The acid dissociation constants of Tl(III) are quite large as compared to Ga(III) or In(III), namely, $K_{a1} = 10^{-1.14}$ and $K_{a2} = 10^{-1.49}$ (3M NaClO₄, 25°C).¹² Measurements were necessarily made at high hydrogen ion concentrations, and ionic strength was adjusted to 2.0. Under the experimental conditions, H_5SXO^+ , H_4SXO , and H_3SXO^- are the predominant charge types of SXO, and we neglected the contribution of $\text{Tl}(\text{OH})_2^+$. The rate constant k_f is expressed as

$$k_f = \frac{[k_{12}[H]^3 + (k_{13}K_2 + k_{22}K_{a1})[H]^2 + (k_{14}K_2K_3 + k_{23}K_2K_{a1})[H] + k_{24}K_3K_4K_{a1}]}{([H] + K_{a1}) \times ([H]^2 + K_2[H] + K_2K_3)}$$

Figure 11 shows the plot of $k_f \times ([H] + K_{a1})([H]^2 + K_2[H] + K_2K_3)$ against $[H]$,¹⁶ giving k_{24} , k_{23} , and k_{14}

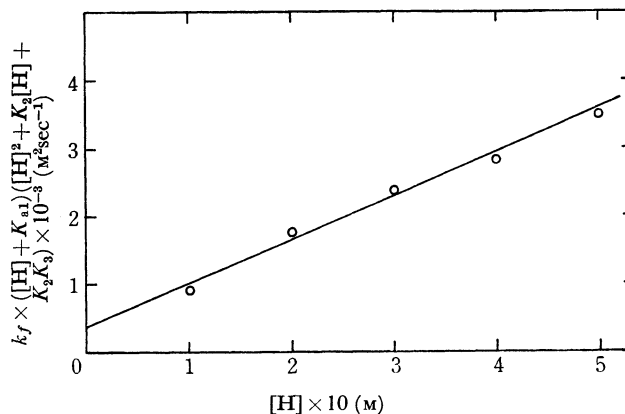


Fig. 11. Plot of $k_f([H] + K_{a1})([H]^2 + K_2[H] + K_2K_3)$ vs. hydrogen ion concentration for Tl(III)-SXO at 25.0°C and ionic strength 2.0.

as 5.3×10^5 , 3.0×10^5 , and $7.0 \times 10^5 \text{ M}^{-1}\text{sec}^{-1}$ respectively.

Unlike the case of Ga(III) or In(III), absorbance of the Tl(III)-SXO complex decreases gradually with time. The complex formation of Tl(III) is, however, much faster than the color fading, and the signals obtained on the screen of the oscilloscope are always exponential curves under the experimental conditions. The rate of color fading increases with decreasing hydrogen ion concentration.

Discussion

The non-linearity of the plot k_{obs} against $[M(\text{III})]$ was interpreted in terms of two-step mechanism including pre-equilibrium (Figs. 2 and 3). Apparent pre-equilibrium constant can be obtained from the slope and the intercept of the plot (Figs. 4 and 5), following the Eq. (2). Apparent pre-equilibrium constants for Ga(III)-SXO and In(III)-SXO are in the order of magnitude of 10^2 M^{-1} . Although this value of K_p is relatively large, ion pair formation constant for 2+ and 2- ions is expected to be of the same order.

It will be difficult to discuss this apparent value of K_p precisely, because the rate equation is not so simple as Eq. (2), when several charge types of the ligand and the metal ions are taken into account; K_p is a function of $[H]$ and k_f is not simply a product of K_p and a constant.

Only the rate constants k_{24} can be discussed among the three metal ions.¹⁷ The order of the values of k_{24} is $\text{InOH}^{2+} > \text{TlOH}^{2+} > \text{GaOH}^{2+}$. The value of k_{24} for Tl(III) is obtained at ionic strength 2.0, whereas that for Ga(III) or In(III) is at ionic strength 0.1. Kinetic measurements for In(III) were also made at ionic strength 2.0. The results are shown in Fig. 10. The concentrations of hydrogen ion were determined by calibrating the measured pH values from ionic strength 2.0 (NaClO₄) to 0.1.

17) The value of k_{24} is indistinguishable from k_{15} as mentioned above, but it seems probable that k_{15} may be neglected. Generally speaking, the rate constants for MOH^{2+} are roughly 10^2 times larger than those for M^{3+} for the same charge type of ligands, as is shown for Fe(III).¹⁴ The values of k_{15} obtained above are close to those of k_{25} . This will be improbable.

16) These were calculated on the added acid concentrations.

TABLE 1. KINETIC RESULTS FOR THE COMPLEX FORMATION OF Ga(III), In(III), AND Tl(III) WITH SXO, AT 25.0°C

	k_{25} M ⁻¹ sec ⁻¹	k_{24} M ⁻¹ sec ⁻¹	k_{15} M ⁻¹ sec ⁻¹	k_{23} M ⁻¹ sec ⁻¹	k_{14} M ⁻¹ sec ⁻¹	I
Ga(III)	1.2×10^4	1.1×10^3	(6.9×10^2)			0.1
In(III)	3.1×10^6	5.0×10^6	(2.8×10^5)			0.1
	10^6	2.2×10^6	(1.3×10^5)			2.0
Tl(III)		5.3×10^5		3.0×10^5	(7.0×10^5)	2.0

In spite of the high NaClO₄ concentration, the pseudo-first-order rate constants k_{obs} are at most three times less than those obtained at ionic strength 0.1 and the results are summarized in Table 1. The order of the values of k_{24} is still that described above, namely, $\text{InOH}^{2+} > \text{TlOH}^{2+} > \text{GaOH}^{2+}$.

As SXO is a multidentate ligand, the complex formation process consists of several steps. The outer-sphere complex must be formed first, regardless of the successive mechanism. An inner-sphere coordinated water molecule is substituted by one of the coordinating groups of SXO next. The dissociation of the water molecule is the rate-determining, if the complex formation proceeds following the Eigen-Tamm mechanism.¹⁾ It seems probable that the first coordination to the metal occurs through one of the carboxyl groups of SXO. The other carboxyl group, the nitrogen of the imino group and the oxygen of the phenol or quinone coordinate to the metal successively. If the pre-equilibrium constant K_p discussed above does not correspond to the ion-pair formation constant, the intermediate $\text{M(III)} \cdots \text{L}$ must be some species formed in these steps. As the coloration of the complex will be resulted from the coordination of the oxygen of the phenol or quinone which is directly connected with the π electron system of the ligand, the intermediate must be formed before the coordination of the phenol oxygen. Then the rate-determining step which may be S_N1 or S_N2 follows; for example the slow cleavage of the hydrogen bond between the imino nitrogen and the phenolic or the quinone oxygen was expected. The measurements of the rate of the proton dissociation reaction was tried by means of the temperature-jump technique. But no signal was observed in our experiment.

Kinetic data to date for trivalent d^{10} -system ions are summarized in Table 2. It is reported that the complex formation of Ga(III) proceeds *via* S_N2 mechanism.^{4,5)} Dividing the rate constant k_{25} for Ga(III)-SXO by ion-

pair formation constant K_{ip} , that is assumed to be 80 ,¹⁸⁾ yields 10^2 sec^{-1} , which is less than the rate constant of the water exchange reaction. The rate constant for Ga^{3+} is lower than that for GaOH^{2+} and then is much lower than that for water substitution reaction of Ga(III). This large difference between the water substitution and the complex formation rate for Ga(III) does not conflict with the S_N2 mechanism. But the fact that the complexing rate for Ga^{3+} is lower than that for GaOH^{2+} , which is also observed in the case of the complex formation with SO_4^{2-} , is inconsistent with the S_N2 mechanism from a coulombic point of view.

The complexing rate of InOH^{2+} with SO_4^{2-} is reported to be $2.5 \times 10^7 \text{ M}^{-1} \text{ sec}^{-1}$.⁴⁾ Assuming the ion-pair formation constant to be 80 M^{-1} , the rate of substitution is $3 \times 10^5 \text{ sec}^{-1}$.

The complexing rate of In^{3+} with murexide is reported to be $2 \times 10^6 \text{ M}^{-1} \text{ sec}^{-1}$.³⁾ As the measurements are carried out at relatively high pH of 3.0–4.4, the contribution of InOH^{2+} must be large. Attributing this rate constant to that for InOH^{2+} , and assuming the ion-pair formation constant to be 5 M^{-1} , first-order rate constant is $4 \times 10^5 \text{ sec}^{-1}$. Estimating the value of ion-pair formation constant for k_{25} and k_{24} to be 80 M^{-1} and 5 M^{-1} respectively, we obtain the first-order rate constants $4 \times 10^4 \text{ sec}^{-1}$ and $1 \times 10^6 \text{ sec}^{-1}$ for k_{25} and k_{24} respectively. So the first-order rate constant for InOH^{2+} is about 10^5 sec^{-1} in every case.

So far as we know, no data have been reported for the rate of complex formation of Tl(III). If the situations for TlOH^{2+} is the same as those for InOH^{2+} mentioned above, *viz.*, the elimination of the coordinated water molecule from the metal ion plays an important role, ionic radius will be a measure of coulombic factor of water elimination. But in effect the order of reactivity is different from that of ionic radius: despite of its larger ionic radius Tl(III) reacts relatively slowly as compared to In(III). This phenom-

TABLE 2. RATE CONSTANTS REPORTED FOR THE COMPLEX FORMATION OF Ga(III) AND In(III) WITH VARIOUS LIGANDS

M(III)	Ga(III)			In(III)		
	Ligand	MTB ^{a)} M ⁻¹ sec ⁻¹	SO_4^{2-} ^{b)} M ⁻¹ sec ⁻¹	OH_2 ^{c)} sec ⁻¹	Murexide ^{d)} M ⁻¹ sec ⁻¹	SO_4^{2-} ^{b)} M ⁻¹ sec ⁻¹
k_f		22.4 (6°C) 40.9 (10°C) 77.1 (15°C)	Ga^{3+} 2.1×10^4 GaOH^{2+} 1.0×10^5	1×10^4	In^{3+} 2.0×10^6	In^{3+} 2.6×10^5
Condition		25°C pH=3.15	25°C $I \rightarrow 0$	25°C	pH=3.0–4.4 12°C, $I=0.1$	InOH^{2+} 2.5×10^7 25°C $I \rightarrow 0$
a) Methylthymol Blue (MTB); Ref. 6. b) Ref. 4. c) Ref. 5. d) Ref. 3.						

18) The values of K_{ip} used here were estimated by using the equation^{19,20)} $K_{ip} = (4Na^3/3000) \exp(-U(a)/RT)$, where N is Avogadro's number, a the encounter complex separation assumed

to be 5 \AA and $U(a)$ the coulombic energy.

19) M. Eigen, *Z. Elektrochem.*, **64**, 115 (1960).

20) R. M. Fuoss, *J. Amer. Chem. Soc.*, **80**, 5059 (1958).

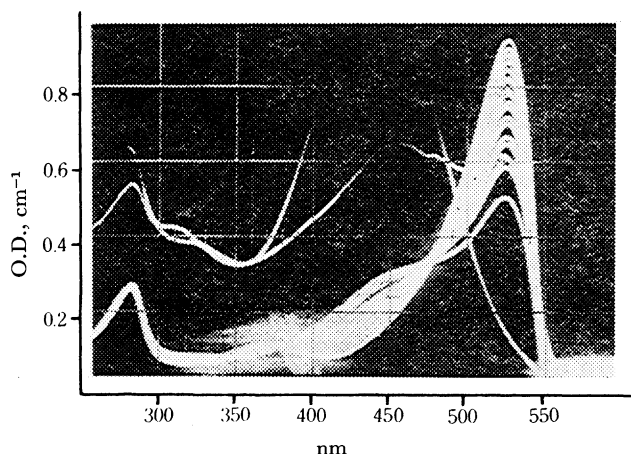


Fig. 12. Change in absorption spectra of Ga(III)-SXO during *ca.* 5 sec after mixing measured by the rapid-scan spectrometer. Each scan needs 300 msec. $[\text{Ga(III)}]_0 = 2.1 \times 10^{-3} \text{ M}$, $[\text{SXO}]_0 = 2.0 \times 10^{-5} \text{ M}$, $\text{pH} = 1.60$, ionic strength 0.1, 25.0°C .

enon may have some relation with the large electron affinity, large acid dissociation constant and relatively large hydration energy of Tl(III). All these properties are interpreted by the large electron attractive force of thallium(III) ion.

The slower increase in absorbance of Ga(III)-SXO complex after the rapid increase is an interesting phenomenon. Figures 12 and 13 show the change of absorption spectrum of Ga(III)-SXO system measured with a rapid-scan spectrophotometer and that measured with a usual spectrophotometer respectively. Isosbestic points are found at 340, 380, and 475 nm in both spectra, and no significant shift of spectra is observed. These results lead us to the mechanism involving only one final product and some slow processes for some of

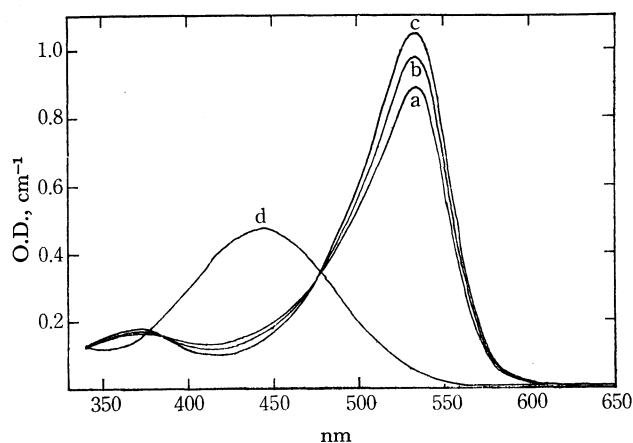


Fig. 13. Slow spectral change of Ga(III)-SXO system at (a): 2 min, (b): 20 min and (c): 600 min after mixing under the same conditions as those in Fig. 12, and (d): the spectrum of SXO.

the reaction components. It would be reasonable to assume that some polymerized or aggregated forms of the reactants may cause such very slow process, though it was not experimentally ascertained. The similar slow processes were also observed in the complex formation between trivalent iron and SXO.

The slow decrease in absorbance in the visible region of Tl(III)-SXO complex is due to the oxidation of SXO by Tl(III), since the similar color fading were also found with the oxidizing agents as Fe(III), Co(III), and Ce(IV), and by anodic oxidation.

The authors wish to thank Professor H. Baba, Research Institute of Applied Electricity of our University, for his permission to use the rapid-scan spectrometer.